Journal of Porphyrins and Phthalocyanines
J. Porphyrins Phthalocyanines 2020; **24**: 817–829
DOI: 10.1142/S1088424619501876

Synthesis of internally alkylated azuliporphyrins

Julian S. D. Moriones, Alissa N. Latham and Timothy D. Lash*◊

Department of Chemistry, Illinois State University, Normal, Illinois 61790-4160, USA

Dedicated to Professor Roberto Paolesse on the occasion of his 60th birthday.

Received 1 September 2019
Accepted 30 November 2019

ABSTRACT: Examples of internally alkylated azuliporphyrins were prepared by MacDonald-type "3 + 1" condensations. 2-Methyl- and 2-ethylazulene reacted with an acetoxymethylpyrrole in the presence of an acid catalyst to give azulitripyrranes. Following cleavage of the terminal protective groups, condensation with a diformylpyrrole in the presence of hydrochloric acid and oxidation with ferric chloride afforded 21-alkylazuliporphyrins. An azulene dialdehyde similarly reacted with an *N*-methyltripyrrane to generate a 23-methylazuliporphyrin. The products could only be isolated in protonated form and the free-base internally alkylated azuliporphyrins proved to be unstable. Nevertheless, the dications are highly diatropic and the internal alkyl group resonances were shifted upfield to beyond -3 ppm. Reaction of a 23-methylazuliporphyrin with palladium(II) acetate primarily afforded a palladium(II) complex with loss of the internal methyl substituent. However, two palladium(II) benzocarbaporphyrins were also identified that were formed by sequential oxidative ring contraction and methyl group migration. Internally alkylated azuliporphyrins provide new insights into the reactivity of the system and the results show that the introduction of alkyl substituents within porphyrinoid cavities greatly modifies the properties of these structures.

KEYWORDS: carbaporphyrins, azuliporphyrins, alkylation, metalation, rearrangements.

INTRODUCTION

The reactivity of porphyrins and related systems can be modified in a number of ways, such as by adding strongly electron-withdrawing or -donating substituents [1], incorporating ring fusion [2–4], reduction [5, 6], core modification [7–10], ring contraction [11–14] and ring expansion [15, 16]. Alkylation of the porphyrin cavity provides an alternative means by which the spectroscopic properties and reactivity of the system can be adjusted [17]. *N*-Alkylporphyrins can be obtained by direct alkylation [18] or by stepwise rational syntheses [19]. Interest in these systems not only derives from their modified characteristics, distorted conformations and altered metalation properties [20], but also from their biological significance [21]. In particular, some drugs can induce cytochrome P-450 enzymes to produce *N*-alkylporphyrins that act as ferrochelatase inhibitors [17, 21]. Alkylation of carbaporphyrinoid structures has also been investigated, including N-confused porphyrins [22–28]. Carbaporphyrin diester **1a** (Fig. 1) reacted with methyl iodide and potassium carbonate to the afford C-alkyl derivative **1b** [23], while benzocarbaporphyrin **2** reacted with alkyl iodides under these conditions to primarily give 22-alkylporphyrinoids **3** together with some of the C-alkylated products **4** [24] (Scheme 1). Oxidized benziporphyrin **5a** [25], tropiporphyrin **6a** [26] and naphthocarbaporphyrin **7a** [27] similarly reacted with methyl iodide to give *N*-alkyl derivatives **5b**, **6b** and **7b**, respectively (Fig. 1), and a carbachlorin has also been reported to give a similar *N*-methyl derivative [28]. Alkylation of **5a** with ethyl iodide afforded the related *N*-ethyl derivative **5c** and it is worth noting that for this series both **5b** and **5c** were obtained as mixtures

---

◊ SPP full member in good standing

*Correspondence to: Timothy D. Lash, tel.: +1 309-438-8554, email: tdlash@ilstu.edu.

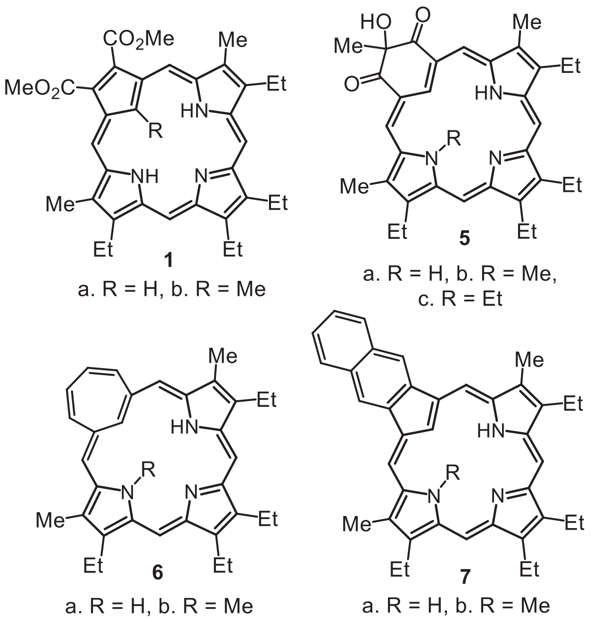

Fig. 1. Selected carbaporphyrinoids and their internally alkylated derivatives

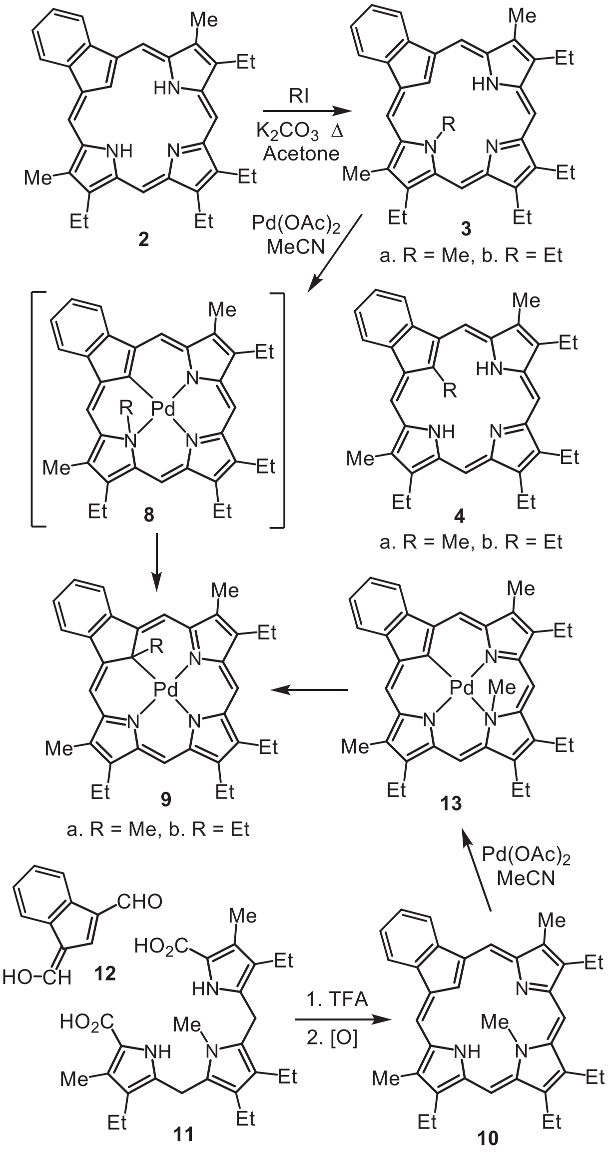

Scheme 1. Synthesis and metalation of internally alkylated carbaporphyrins

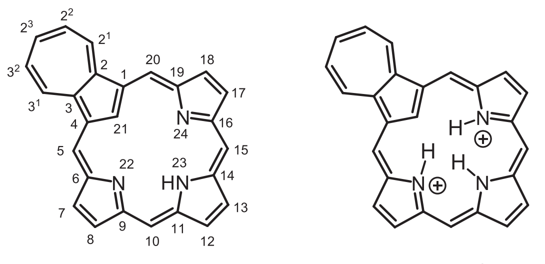

Fig. 2. Structures of azuliporphyrin and the related dication

of diastereoisomers [25]. Nevertheless, in all of these reactions, *N*-substitution only takes place on the pyrrolic units adjacent to the carbocyclic rings.

N-Alkylbenzocarbaporphyrins **3a** and **3b** were found to react with palladium(II) acetate in refluxing acetonitrile to give palladium(II) complexes [24, 29]. Although *N*-alkyl complexes **8** were initially generated, rapid alkyl group migration took place to afford C-alkyl products **9** (Scheme 1). In order to further investigate this phenomenon, 23-methylbenzocarbaporphyrin **10** was prepared by the "3 + 1" version of the MacDonald condensation from *N*-methyltripyrrane **11** and indene dialdehyde **12** [29]. Subsequent reaction with palladium(II) acetate initially generated *N*-methyl complex **13**, but this also underwent alkyl group migration, albeit at a much slower rate, to afford **9a** (Scheme 1). It was proposed that a transient palladium(IV) alkyl complex was involved in mediating these transformations [29]. It is noteworthy that internal alkylation of porphyrinoid systems induces bathochromic shifts to the UV-vis spectra and substantially alters the metalation chemistry for these macrocycles [17]. In addition, the presence of alkyl substituents differentiates between the two faces of the macrocycle and this breaks the symmetry of these systems resulting in the formation of chiral structures.

Azuliporphyrins **14** (Fig. 2) are an unusual family of porphyrin analogues that incorporate an azulene unit in place of one of the pyrrole rings [30, 31]. Compared to true carbaporphyrins such as **2** [32, 33], azuliporphyrins have substantially reduced aromatic characteristics but nevertheless still retain recognizable global diatropicity [30, 34]. The proton NMR spectra of azuliporphyrins show the *meso*-carbons near 8 and 9 ppm, compared to *ca*. 10 ppm in *meso*-unsubstituted porphyrins and carbaporphyrins [31, 35]. Addition of trifluoroacetic acid (TFA) to solutions of azuliporphyrins generates the related dications **14**H_2^{2+}, and these show substantially increased diatropic character [31, 35]. As is the case for other carbaporphyrinoid systems, including N-confused porphyrins [36], azuliporphyrins readily form stable organometallic derivatives [37, 38]. Copper(II) salts promote oxidative metalations to give copper(II) oxyazuliporphyrins [39], while peroxides induce ring contractions to afford benzocarbaporphyrins [40, 41]. The rich and unusual reactivity of azuliporphyrins has led to the exploration of related systems such as azulichlorins [42], azulisapphyrin [43], azulicorrole [44], and other conjugated azulene-containing structures [45]. However, our attempts to modify the properties of azuliporphyrins by alkylation of the inner core have been unsuccessful. In order to assess how alkylation affects the reactivity and spectroscopic properties of this system, two stepwise routes to internally alkylated azuliporphyrins have been developed and these investigations are detailed below.

EXPERIMENTAL

Melting points are uncorrected. NMR spectra were recorded using a 400 or 500 MHz NMR spectrometer and were run at 302 K unless otherwise indicated. ^{1}H NMR values are reported as chemical shifts δ, relative integral, multiplicity (*s*, singlet; *d*, doublet; *t*, triplet; *q*, quartet; *m*, multiplet; br, broad peak) and coupling constant (*J*). Chemical shifts are reported in parts per million (ppm) relative to $CDCl_3$ (^{1}H residual $CHCl_3$ δ 7.26, ^{13}C $CDCl_3$ triplet δ 77.23) and coupling constants were taken directly from the spectra. NMR assignments were made with the aid of ^{1}H–^{1}H COSY, HSQC, DEPT-135 and NOE difference proton NMR spectroscopy. 2D experiments were performed by using standard software. ^{1}H and ^{13}C NMR spectra for all new compounds are reported in the supplementary materials.

3-*Acetyl*-2*H*-*cyclohepta*[*b*]*furan*-2-*one* (16*a*). A solution of sodium ethoxide, prepared by reacting sodium (0.81 g) with ethanol (60 mL), was added to a stirred suspension of tropolone *p*-toluenesulfonate [46] (8.07 g, 29.2 mmol) in ethyl acetoacetate (6.2 mL, 6.3 g, 48 mmol) and ethanol (30 mL) at 0 °C. The mixture was stirred for 16 h at room temperature and then heated at 50 °C for 45 min. Water (100 mL) was added and the resulting precipitate collected by suction filtration. The solid was washed with water and dried *in vacuo* to give the product (4.61 g, 24.5 mmol, 84%) as a yellow solid, mp 205.5–206.5 °C (lit. mp [47] 206 °C; 206–207 °C [48]). ^{1}H NMR (500 MHz, $CDCl_3$): δ 2.63 (3H, s, CH_3), 7.38–7.44 (1H, m), 7.53–7.58 (2H, m), 7.66–7.70 (1H, m), 9.19 (1H, d, *J* = 11.3 Hz, 4-H). ^{13}C{H} NMR (125 MHz, $CDCl_3$): δ 30.2 (CH_3), 103.9, 120.2 (CH), 132.0 (CH), 135.2 (CH), 136.7 (CH), 141.0 (CH), 153.5, 159.4, 167.7 (CO_2H), 195.3 (ketone-C=O).

3-*Propionyl*-2*H*-*cyclohepta*[*b*]*furan*-2-*one* (16*b*). Tropolone *p*-toluenesulfonate (8.07 g, 29.2 mmol) was reacted with ethyl propionylacetate (6.2 mL, 6.3 g, 43 mmol) under the foregoing conditions to give the title compound (3.51 g, 17.4 mmol, 59%) as a yellow solid, mp 130.5–131.5 °C. ^{1}H NMR (500 MHz, $CDCl_3$): δ 1.89 (3H, t, *J* = 7.3 Hz, CH_2CH_3), 3.07 (2H, q, *J* = 7.3 Hz, CH_2CH_3), 7.36–7.41 (1H, m), 7.51–7.56 (2H, m), 7.64–7.69 (1H, m), 9.22 (1H, d, *J* = 11.3 Hz, 4-H); ^{13}C{H} NMR (125 MHz, $CDCl_3$): δ 7.9 (CH_2CH_3), 35.3 (CH_2CH_3), 103.3, 120.0 (CH), 131.7 (4-CH), 135.0 (CH), 136.5 (CH), 140.7 (CH), 153.5, 159.2, 167.4 (CO_2H), 198.2 (ketone-C=O).

1-*Cyano*-2-*methylazulene*-3-*carboxylic acid* (17*a*). A solution of sodium ethoxide, prepared by reacting sodium (1.65 g) with ethanol (80 mL), was added to a stirred mixture of **16a** (3.62 g, 19.2 mmol) and ethyl cyanoacetate (3.8 mL, 4.0 g, 36 mmol) in ethanol. After stirring at room temperature for 16 h, water was added and the mixture washed with dichloromethane. Hydrochloric acid (1 M, 50 mL) was added to the aqueous layer, and the resulting precipitate was collected by suction filtration and washed with water. The solid was dried in a vacuum desiccator overnight to give the carboxylic acid (3.56 g, 16.9 mmol, 88%) as a salmon-pink solid, mp 262–264 °C, dec. (lit. mp [49] 273 °C). ^{1}H NMR (500 MHz, $CDCl_3$): δ 2.85 (3H, s, 2-Me), 7.92 (1H, t, *J* = 9.7 Hz, 5-H), 7.96 (1H, t, *J* = 10.0 Hz, 7-H), 8.15 (1H, t, *J* = 9.8 Hz, 6-H), 8.64 (1H, d, *J* = 9.7 Hz, 4-H), 9.62 (1H, d, *J* = 10.1 Hz). ^{13}C{H} NMR (125 MHz, $CDCl_3$): δ 16.6 (2-Me), 98.3, 116.2 (CN), 131.4 (5-CH), 132.1 (7-CH), 136.2 (4-CH), 138.7 (8-CH), 141.3 (6-CH), 142.3, 144.1, 156.3, 165.9 (CO_2H).

1-*Cyano*-2-*ethylazulene*-3-*carboxylic acid* (17*b*). 16b (3.62 g, 17.9 mmol) and ethyl cyanoacetate (3.8 mL, 4.0 g, 36 mmol) were reacted under the previous conditions to give the azulene carboxylic acid (2.59 g, 11.5 mmol, 64%) as a salmon-pink solid, mp 231–233 °C with softening at 220 °C. ^{1}H NMR (500 MHz, $CDCl_3$): δ 1.29 (3H, t, *J* = 7.5 Hz, CH_2CH_3), 3.28 (2H, q, *J* = 7.3 Hz, 2-CH_2), 7.92 (1H, dt, *J* = 0.9, 9.7 Hz, 5-H), 7.95 (1H, dt, *J* = 0.9, 10.0 Hz, 7-H), 8.15 (1H, tt, *J* = 1.1, 9.8 Hz, 6-H), 8.65 (1H, dt, *J* = 1.1, 9.7 Hz, 4-H), 9.61 (1H, dt, *J* = 1.0, 10.1 Hz), 12.95 (1H, br s, OH). ^{13}C{H} NMR (125 MHz, $CDCl_3$): δ 15.3 (CH_2CH_3), 23.1 (CH_2CH_3), 97.3, 115.5, 116.1, 131.4 (5-CH), 132.0 (7-CH), 136.4 (4-CH), 139.0 (8-CH), 141.4 (6-CH), 142.4, 144.3, 162.0, 165.8 (CO_2H).

2-*Methylazulene* (18*a*). The foregoing carboxylic acid (3.70 g, 17.5 mmol) was added to a 75% aqueous solution of sulfuric acid and heated for 2 h at 90 °C and then 120 °C for a further 2 h. The mixture was cooled and poured into a solution of sodium hydroxide (35 g) in water (50 mL). The mixture was extracted with hexanes and ethyl acetate, washed with water, and the solvent removed on a rotary evaporator. The residue was purified by column chromatography on silica gel, eluting with hexanes, and the product eluted as a blue fraction. Evaporation of the solvent gave 2-methylazulene (1.33 g, 9.37 mmol, 53%) as dark-purple crystals, mp 49–50.5 °C (lit. mp [50] 49–50 °C). ^{1}H NMR (500 MHz, $CDCl_3$):

δ2.68 (3H, s, 2-Me), 7.15 (2H, t, *J* = 9.8 Hz, 5,7-H), 7.20 (2H, s, 1,3-H), 7.50 (1H, t, *J* = 9.9 Hz, 6-H), 8.20 (2H, d, *J* = 9.6 Hz, 4,8-H). ^{13}C{H} NMR (125 MHz, $CDCl_3$): δ 16.9 (2-Me), 118.5 (1,3-CH), 123.2 (5,7-CH), 134.3 (4,8-CH), 135.6 (6-CH), 140.9 (2-C), 150.6 (3a,8a-C).

***2-Ethylazulene* (18*b*).** Treatment of **17b** (2.00 g, 8.89 mmol) with sulfuric acid using the procedure given above afforded 2-ethylazulene (0.67 g, 4.3 mmol, 48%) as dark purple crystals, mp 44–45 °C (lit. mp [51] 44.5 °C; 43–44 °C [52]). ^{1}H NMR (500 MHz, $CDCl_3$): δ 1.43 (3H, t, *J* = 7.6 Hz, $\mathrm{CH_2C}H_3$), 3.05 (2H, q, *J* = 7.6 Hz, $\mathrm{C}H_2\mathrm{CH_3}$), 7.15 (2H, t, *J* = 9.8 Hz, 5,7-H), 7.25 (2H, s, 1,3-H), 7.51 (1H, t, *J* = 9.9 Hz, 6-H), 8.22 (2H, d, *J* = 9.6 Hz, 4,8-H). ^{13}C{H} NMR (125 MHz, $CDCl_3$): δ 14.8 ($\mathrm{CH_2}C\mathrm{H_3}$), 24.5 ($C\mathrm{H_2CH_3}$), 117.0 (1,3-CH), 123.2 (5,7-CH), 134.6 (4,8-CH), 135.6 (6-CH), 140.8 (6-C), 157.1 (3a,8a-C).

1,3-*Bis*-(5-*tert*-*butoxycarbonyl*-3-*ethyl*-4-*methyl*-2-*pyrrolylmethyl*)-2-*methylazulene* (20*a*). A solution of 2-methylazulene (100 mg, 0.704 mmol) and *tert*-butyl 5-acetoxymethyl-4-ethyl-3-methylpyrrole-2-carboxylate [53] (435 mg, 1.55 mmol) in dichloromethane (46 mL) was vigorously stirred with K 10 Montmorillonite clay (0.70 g) at room temperature under nitrogen for 16 h. The mixture was suction filtered and the clay washed with dichloromethane. The solvent was evaporated under reduced pressure and the residue purified on a silica gel column, eluting with 20% hexanes-dichloromethane. The deep-blue product fraction was recrystallized from chloroform-hexanes to give the azulitripyrrane (310 mg, 0.530 mmol, 75%) as a blue powder, mp 184–185.5 °C (rapid heating gave a mp of *ca.* 140 °C). ^{1}H NMR (500 MHz, $CDCl_3$): δ1.15 (6H, t, *J* = 7.5 Hz, 2 × $\mathrm{CH_2C}H_3$), 1.44 (18H, s, 2 × O*t*-Bu), 2.25 (6H, s, 2 × pyrrole-CH_3), 2.35 (3H, 2-CH_3), 2.56 (4H, q, *J* = 7.5 Hz, 2 × $\mathrm{C}H_2\mathrm{CH_3}$), 4.31 (4H, s, 2 × bridge-CH_2), 7.10 (2H, t, *J* = 9.9 Hz), 7.51 (1H, t, *J* = 9.8 Hz), 7.87 (2H, br s, 2 × NH), 8.12 (2H, d, *J* = 9.7 Hz). ^{13}C{H} NMR (125 MHz, $CDCl_3$): δ 10.7 (2 × pyrrole-Me), 13.2 (2-Me), 15.6 (2 × $\mathrm{CH_2}C\mathrm{H_3}$), 17.6 (2 × $C\mathrm{H_2CH_3}$), 22.3 (2 × bridge-CH_2), 28.7 (2 × *t*-Bu), 80.2 (2 × O-*C*Me$_3$), 118.6, 122.5, 122.97, 123.02, 125.9, 131.4 (4,8-CH), 131.7, 136.7 (6-CH), 137.4, 147.9, 161.6. HRMS (ESI) *m/z*: [M + H]$^+$ calcd. for $C_{37}H_{49}N_2O_4$ 585.3687; found 585.3676.

1,3-*Bis*-(5-*tert*-*butoxycarbonyl*-3-*ethyl*-4-*methyl*-2-*pyrrolylmethyl*)-2-*ethylazulene* (20*b*). 2-Ethylazulene (110 mg, 0.705 mmol) was reacted with **19** [53] (435 mg, 1.55 mmol) under the foregoing conditions. Following column chromatography, eluting with 20% hexanes-dichloromethane, and recrystallization from chloroform-hexanes, the azulitripyrrane (344 mg, 0.574 mmol, 82%) was obtained as a blue powder, mp 173.5–174.5 °C. ^{1}H NMR (500 MHz, $CDCl_3$): δ 0.97 (3H, t, *J* = 7.6 Hz, 2-$\mathrm{CH_2C}H_3$), 1.16 (6H, t, *J* = 7.5 Hz, 2 × pyrrole-$\mathrm{CH_2C}H_3$), 1.44 (18H, s), 2.25 (6H, s, 2 × pyrrole-CH_3), 2.57 (4H, q, *J* = 7.5 Hz, 2 × pyrrole-CH_2), 2.79 (2H, q, *J* = 7.6 Hz, 2-CH_2), 4.32 (4H, s, 2 × bridge-CH_2), 7.10 (2H, t, *J* = 9.9 Hz, 5,7-H), 7.51 (1H, t, *J* = 9.8 Hz, 6-H), 7.87 (2H, br s, 2 × NH), 8.12 (2H, d, *J* = 9.8 Hz, 4,8-H). ^{13}C{H} NMR (125 MHz, $CDCl_3$): δ 10.7 (2 × pyrrole-CH_3), 15.0 (2-$\mathrm{CH_2}C\mathrm{H_3}$), 15.6 (2 × pyrrole-$\mathrm{CH_2}C\mathrm{H_3}$), 17.6 (2 × pyrrole-$CH_2$), 21.0 (2-$CH_2$), 22.1 (2 × bridge-$CH_2$), 28.7 (*t*-Bu), 80.1 (O-*C*Me$_3$), 118.5, 121.8, 122.9, 123.0 (5,7-CH), 125.9, 131.6, 132.0 (4,8-CH), 136.8 (6-CH), 137.7, 153.9, 161.6. HRMS (ESI) *m/z*: [M + H]$^+$ calcd. for $C_{38}H_{51}N_2O_4$ 599.3843; found 599.3832.

7,12,13,18-*Tetraethyl*-8,17,21-*trimethylazuliporphyrin dihydrochloride* (23*a*·2*HCl*). In a 100 mL pear-shaped flask, TFA (3 mL) was added to azulitripyrrane **20a** (99 mg, 0.17 mmol) and the mixture stirred for 10 min under nitrogen. The TFA was evaporated, the residue dissolved in acetic acid, and pyrrole dialdehyde **21** [54, 55] (32 mg, 0.18 mmol) was added. Conc. hydrochloric acid (10 drops) was immediately added and the mixture stirred overnight under nitrogen at room temperature. The solution was diluted with dichloromethane (100 mL) and shaken vigorously with 0.1% aqueous ferric chloride solution for 5 min. The organic layer was separated, and the aqueous solution back extracted with dichloromethane. The combined organic layers were washed sequentially with water, saturated sodium bicarbonate, and 10% hydrochloric acid. The organic phase was dried over sodium sulfate, filtered, and evaporated under reduced pressure. The residue was recrystallized twice with chloroform-hexanes to give the protonated azuliporphyrin (62 mg, 0.10 mmol, 61%) as dark-green crystals, mp >300 °C, dec. UV-vis ($CHCl_3$): λ_{max}/nm (log ε) 336 (sh, 4.40), 376 (4.56), 457 (4.63), 494 (sh, 4.34), 647 (4.17), 682 (4.11), 737 (sh, 3.78). UV-vis (1% TFA-$CHCl_3$): λ_{max}/nm (log ε) 374 (4.62), 460 (4.67), 490 (sh, 4.43), 655 (4.18), 679 (4.17), 731 (sh, 3.84). UV-vis (1% Et_3N-$CHCl_3$): λ_{max}/nm (log ε) 373 (4.50), 416 (sh, 4.45), 437 (4.46), 463 (4.39), 583 (4.00), 639 (sh, 3.92). ^{1}H NMR (500 MHz, $CDCl_3$): δ -3.62 (3H, s, 21-CH_3), 1.61 (6H, t, *J* = 7.6 Hz), 1.68 (6H, t, *J* = 7.6 Hz) (4 × $\mathrm{CH_2C}H_3$), 3.27 (6H, s, 7,18-CH_3), 3.56–3.61 (4H, m), 3.80–3.87 (2H, m), 3.96–4.04 (2H, m) (8,12,13,17-CH_2), 8.18–8.25 (3H, m, 2^2,2^3,3^2-H), 8.99 (2H, s, 10,15-H), 9.85 (2H, d, *J* = 9.8 Hz, 2^1,3^1-H), 10.23 (2H, s, 5,20-H). ^{13}C NMR (partial data from HSQC spectrum, $CDCl_3$): δ 10.3 (7,18-Me), 12.6 (21-Me), 16.7 (2 × $\mathrm{CH_2}C\mathrm{H_3}$), 17.5 (2 × $\mathrm{CH_2}C\mathrm{H_3}$), 18.3 (2 × $C\mathrm{H_2CH_3}$), 18.6 (2 × $C\mathrm{H_2CH_3}$), 95.4 (10,15-CH), 107.0 (5,20-CH), 137.1 (2^1,3^1-CH), 137.7 (2^2,3^2-CH). HRMS (ESI) *m/z*: [M + H]$^+$ calcd. for $C_{37}H_{40}N_3$ 526.3217; found 526.3206.

7,12,13,18,21-*Pentaethyl*-8,17-*dimethylazuliporphyrin dihydrochloride* (23*b*·2*HCl*). Azulitripyrrane **20b** (105 mg, 0.175 mmol) was reacted with dialdehyde **21** (32 mg, 0.18 mmol) under the previous conditions. The product was recrystallized twice from chloroform-hexanes to give **23b**·2HCl (66 mg, 0.11 mmol, 62%) as dark-green crystals, mp > 300 °C. UV-vis ($CHCl_3$): λ_{max}/nm (log ε) 337 (sh, 4.37), 376 (4.52), 458 (4.61), 645 (4.14), 684 (sh, 4.05), 740 (sh, 3.76). UV-vis (1% TFA-$CHCl_3$): λ_{max}/nm (log ε) 336 (sh, 4.35), 374 (4.60), 464

(4.67), 654 (4.14), 680 (sh, 4.12), 735 (sh, 3.78). UV-vis (1% Et_3N-$CHCl_3$): λ_{max}/nm (log ε) 375 (4.46), 436 (4.46), 462 (4.39), 586 (3.91), 641 (sh, 3.84). ^{1}H NMR (500 MHz, $CDCl_3$): δ -3.79 (2H, br q, 21-$C\mathit{H}_2CH_3$), -2.01 (3H, br t, $CH_2C\mathit{H}_3$), 1.61–1.68 (12H, m, 4 × $CH_2C\mathit{H}_3$), 3.29 (6H, s, 7,18-CH_3), 3.56–3.63 (4H, m), 3.81–3.88 (2H, m), 4.01–4.08 (2H, m) (8,12,13,17-CH_2), 8.19–8.27 (3H, m, $2^2,2^3,3^2$-H), 9.02 (2H, s, 10,15-H), 9.91 (2H, br d, *J* = 9.1 Hz, $2^1,3^1$-H), 10.32 (2H, s, 5,20-H). ^{13}C NMR (partial data from HSQC spectrum, $CDCl_3$): δ 9.4 (21-$CH_2\mathit{C}H_3$), 10.3 (7,18-Me), 16.8 (2 × $CH_2\mathit{C}H_3$), 17.4 (2 × $CH_2\mathit{C}H_3$), 18.3 (2 × $\mathit{C}H_2CH_3$), 18.5 (21-CH_2), 18.6 (2 × $\mathit{C}H_2CH_3$), 95.4 (10,15-CH), 107.8 (5,20-CH), 137.1 ($2^1,3^1$-CH), 137.4 ($2^2,3^2$-CH), 143.3 (2^3-CH). HRMS (ESI) *m/z*: $[M + H]^+$ calcd. for $C_{38}H_{42}N_3$ 540.3373; found 540.3360.

2^3-*tert-Butyl*-7,12,13,18-*tetraethyl*-8,17-*dimethylazuliporphyrin dihydrochloride* (24*b* · 2*HCl*). *N*-methyl tripyrrane **11** [29] (103 mg, 0.221 mmol) was dissolved in TFA (1 mL) and stirred for 2 min under nitrogen. The mixture was diluted with dichloromethane (99 mL), followed by the immediate addition of 6-*tert*-butylazulene-1,3-dicarbaldehyde [56] (57.6 mg, 0.240 mmol), and the solution was left to stir overnight under nitrogen. The mixture was vigorously shaken with aqueous ferric chloride solution (0.1%, 200 mL), and then washed with 10% aqueous hydrochloric acid. The solvent was evaporated off under reduced pressure and the residue was recrystallized twice from chloroform-hexanes to give the *tert*-butyl *N*-methylazuliporphyrin dihydrochloride (113 mg, 0.172 mmol, 78%) as dark crystals, mp >300 °C. UV-vis ($CHCl_3$): λ_{max}/nm (log ε) 377 (4.56), 449 (sh, 4.51), 476 (4.81), 592 (4.00), 648 (4.26), 697 (sh, 3.93), 757 (sh, 3.69). UV-vis (1% TFA-$CHCl_3$): λ_{max}/nm (log ε) 371 (4.65), 444 (sh, 4.57), 470 (4.85), 590 (4.04), 648 (4.29), 747 (sh, 3.77). UV-vis (1% Et_3N-$CHCl_3$): λ_{max}/nm (log ε) 364 (4.58), 402 (4.56), 457 (4.53), 484 (4.61), 630 (sh, 3.96), 669 (sh, 4.53). ^{1}H NMR (500 MHz, TFA-d_6-DMSO): δ -3.54 (1H, s, CH), -3.48 (3H, s, N-Me), -0.57 (2H, br s, 2 × NH), 1.16 (6H, t, *J* = 7.6 Hz) 1.46 (6H, t, *J* = 7.6 Hz) (4 × $CH_2C\mathit{H}_3$), 1.52 (9H, s, *t*-Bu), 3.33 (6H, s, 7,18-Me), 3.35–3.42 (2H, m), 3.48–3.55 (2H, m), 3.64–3.76 (4H, m), (4 × $C\mathit{H}_2CH_3$), 8.77 (2H, d, *J* = 10.7 Hz, 2^2, 3^2-CH), 9.46 (2H, s, 10,15-H), 10.09 (2H, d, *J* = 10.7 Hz, 2^1, 3^1-CH), 10.44 (2H, s, 5,20-H). ^{13}C{^{1}H} NMR (125 MHz, TFA-d_6-DMSO, 60 °C): δ 11.8 (7,18-Me), 16.4 (2 × CH_2CH_3), 16.7 (2 × $CH_2\mathit{C}H_3$), 19.75 (2 × $\mathit{C}H_2CH_3$), 19.78 (2 × $\mathit{C}H_2CH_3$), 31.7 ($C(\mathit{C}H_3)_3$), 32.4 (N-Me), 41.0 ($\mathit{C}(CH_3)_3$), 97.3 (10,15-CH), 111.2 (5,20-CH), 125.8 (21-CH), 129.4, 141.2, 141.6 ($2^1,3^1$-CH), 141.7, 142.2, 142.4 ($2^2,3^2$-CH), 142.5, 146.4, 153.9, 156.9, 174.2. HR-MS (ESI) m/z: $[M + H]^+$ calcd for $C_{41}H_{48}N_3$ 582.3848, found 582.3847.

***Reaction of* 24*b with palladium*(II) *acetate*.** 23-Methylazuliporphyrin **24b** · 2HCl (20.0 mg, 0.0305 mmol) was stirred under reflux with palladium(II) acetate (15.0 mg) in a 50/50 mixture of acetonitrile-chloroform (30 mL) for 16 h. The solvent was removed under reduced pressure and the residue purified on a silica column eluting with 50% dichloromethane-hexanes. A pale green fraction was collected, followed by a major green-brown fraction corresponding to palladium(II) complex **26**. A third fraction was subsequently collected that corresponded to palladium(II) carbaporphyrin carbaldehyde **28b** (1.0 mg, 0.0015 mmol, 5.0%). The major product was recrystallized from chloroform-methanol to give **26** (9.2 mg, 0.0137 mmol, 45%) as a dark solid, mp >300 °C. Fraction 1 was further purified on silica, eluting with 25% dichloromethane-hexanes and afforded palladium(II) *tert*-butylbenzocarbaporphyrin **28a** (0.5 mg, 0.00074 mmol, 2.4%) as a dark solid.

(2^3-*tert-Butyl*-8,12,13,17-*tetraethyl*-7,18-*dimethylazuliporphyrinato*)*palladium*(II) (26). UV-vis ($CHCl_3$): λ_{max}/nm (log ε) 366 (4.62), 415 (4.52), 448 (4.51), 508 (sh, 3.91), 569 (4.20), 659 (3.97), 732 (sh, 3.64). ^{1}H NMR (500 MHz, $CDCl_3$): δ1.57 (9H, s, *t*-Bu), 1.66 (6H, t, *J* = 7.7 Hz), 1.70 (6H, t, *J* = 7.7 Hz) (4 × $CH_2C\mathit{H}_3$), 3.16 (6H, s, 7,18-Me), 3.51–3.58 (8H, m, 4 × $C\mathit{H}_2CH_3$), 7.75 (2H, d, *J* = 10.8 Hz, $2^2,3^2$-H), 8.68 (2H, s, 10,15-H), 9.03 (2H, d, *J* = 10.8 Hz, $2^1,3^1$-H), 9.26 (2H, s, 5,20-H). ^{13}C{H} NMR (125 MHz, $CDCl_3$): δ 11.2 (7,18-CH_3), 16.7 (2 × pyrrole-$CH_2\mathit{C}H_3$), 17.6 (2 × pyrrole-$CH_2\mathit{C}H_3$), 19.3 (2 × pyrrole-CH_2), 19.7 (2 × pyrrole-CH_2), 31.7 (*t*-Bu), 38.8 (*C*Me$_3$), 96.4 (10,15-CH), 108.6 (5,20-CH), 125.3, 130.2 ($2^1,3^1$-CH), 133.6 ($2^2,3^2$-CH), 136.2, 140.5, 142.8, 142.9, 147.2, 148.7, 152.8, 159.7, 161.6. HRMS (ESI) *m/z*: $[M + H]^+$ calcd. for $C_{40}H_{44}N_3Pd$ 672.2570; found 672.2586.

(2^2-*tert-Butyl*-7,12,13,18-*tetraethyl*-8,17,21-*trimethylbenzo*[*b*]*carbaporphyrinato*)*palladium*(II) (28*a*). UV-vis ($CHCl_3$): λ_{max}/nm (relative intensity) 348 (0.68), 423 (1.00), 633 (sh, 0.185), 694 (0.37). ^{1}H NMR (500 MHz, $CDCl_3$): δ -3.24 (3H, s, 21-Me), 1.73–1.77 (21H, m, 4 × $CH_2C\mathit{H}_3$ and *t*-Bu), 3.33 (3H, s), 3.36 (3H, s) (7,18-Me), 3.72–3.78 (8H, m, 4 × $C\mathit{H}_2CH_3$), 8.34 (1H, d, *J* = 8.5 Hz, 3^2-H), 9.32 (1H, d, *J* = 8.5 Hz, 3^1-H), 9.36 (1H, s, 2^1-H), 9.55 (1H, s), 9.56 (1H, s) (10,15-H), 10.22 (1H, s), 10.27 (1H, s) (5,20-H). HRMS (ESI) *m/z*: $[M + H]^+$ calcd. for $C_{40}H_{46}N_3Pd$ 674.2726; found 674.2757.

(7,12,13,18-*Tetraethyl*-2^2-*formyl*-8,17,21-*trimethylbenzo*[*b*]*carbaporphyrinato*)*palladium*(II) (28*b*). UV-vis ($CHCl_3$): λ_{max}/nm (relative intensity) 346 (0.79), 429 (1.00), 520 (sh, 0.30), 648 (sh, 0.15), 715 (0.32). ^{1}H NMR (500 MHz, $CDCl_3$): δ -3.20 (3H, s, 21-Me), 1.76 (12H, m, 4 × $CH_2C\mathit{H}_3$), 3.34 (3H, s), 3.35 (3H, s) (7,18-Me), 3.72–3.79 (8H, m, 4 × $C\mathit{H}_2CH_3$), 8.71 (1H, d, *J* = 8.2 Hz, 3^2-H), 9.50 (1H, d, *J* = 8.2 Hz, 3^1-H), 9.58 (1H, s), 9.61 (1H, s) (10,15-H), 9.90 (1H, s, 2^1-H), 10.36 (1H, s), 10.39 (1H, s) (5,20-H), 10.64 (1H, s, CHO). ^{13}C NMR (partial data from HSQC spectrum, $CDCl_3$): δ 11.48, 11.53 (7,18-Me), 17.46, 17.50 (4 × $CH_2\mathit{C}H_3$), 18.31, 18.33 (4 × $\mathit{C}H_2CH_3$), 19.3, 19.8 (4 × $\mathit{C}H_2CH_3$), 23.4 (21-Me), 106.6, 107.0 (10,15-CH), 107.2, 109.0 (5,20-CH), 123.0

(3^1-CH), 126.1 (2^1-CH), 126.6 (3^2-CH), 193.0 (CHO). HRMS (ESI) *m/z*: [M + H]$^+$ calcd. for $C_{37}H_{38}N_3OPd$ 645.2050; found 646.2047.

Reaction of* 23a *with palladium*(II) *acetate. 21-Methylazuliporphyrin **23a**·2HCl (20.0 mg, 0.0305 mmol) was reacted with palladium(II) acetate under the foregoing conditions. The crude products were run through a silica gel column, eluting with 50% dichloromethane-hexanes. The initial dark brown band corresponded to a mixture of aromatic products. A second green-brown band was collected that gave palladium(II) complex **35** (2.1 mg, 0.0034 mmol, 11%) as a dark solid, mp > 300 °C.

(7,12,13,18-*Tetraethyl*-8,17-*dimethylazuliporphyrinato*)*palladium*(II) (35). UV-vis ($CHCl_3$): λ_{max}/nm (log ε) 368 (4.72), 413 (4.68), 447 (4.61), 511 (sh, 3.99), 574 (4.34), 667 (sh, 4.02), 740 (3.70). ^{1}H NMR (500 MHz, $CDCl_3$): δ 1.66–1.70 (12H, 2 overlapping triplets, *J* = 7.7 Hz, 4 × CH_2CH_3), 3.07 (6H, s, 8,17-Me), 3.51 (4H, q, *J* = 7.7 Hz), 3.61 (4H, q, *J* = 7.7 Hz) (4 × CH_2CH_3), 7.48–7.53 (3H, m, 2^2,2^3,3^2-H), 8.61 (2H, s, 10,15-H), 9.01–9.04 (2H, m, 2^1,3^1-H), 9.22 (2H, s, 5,20-H). ^{13}C{H} NMR (125 MHz, $CDCl_3$): δ 11.4 (8,17-CH_3), 17.4 (2 × pyrrole-CH_2CH_3), 17.6 (2 × pyrrole-CH_2CH_3), 19.2 (2 × pyrrole-CH_2), 19.5 (2 × pyrrole-CH_2), 96.4 (10,15-CH), 108.6 (5,20-CH), 125.2, 130.6 (2^1,3^1-CH), 133.5, 135.1 (2^2,3^2-CH), 137.6 (2^3-CH), 142.2, 143.0, 143.6, 147.7, 150.1, 153.4.

RESULTS AND DISCUSSION

Initial investigations were directed towards the synthesis of 21-alkylated azuliporphyrins from 2-methyl- and 2-ethylazulene using the "3 + 1" version of the MacDonald condensation [57, 58]. The required azulenes were prepared by adapting procedures reported by Iwama *et al*. [59]. Tropolone *p*-toluene sulfonate (**15**) reacted with ethyl acetoacetate in the presence of sodium ethoxide to give 3-acetylcycloheptafuranone **16a** in 84% yield (Scheme 2). Similarly, reaction of **15** with ethyl propionylacetate afforded the related propionyl derivative **16b**. Reaction of **16a** and **16b** with ethyl cyanoacetate and sodium ethoxide then led to the formation of 3-cyanoazulene-1-carboxylic acids **17a** and **17b**. Finally, hydrolysis of the nitrile substituent and decarboxylation with 75% sulfuric acid generated 2-alkylazulenes **18a** and **18b**. Azulene and 6-substituted azulenes have previously been shown to react with acetoxymethylpyrroles such as **19** in the presence of acetic acid in refluxing alcohol solvents to give azulitripyrranes [35, 56, 60]. Alternatively, the reaction can be catalyzed by K 10 Montmorillonite clay in dichloromethane at room temperature [61]. The latter procedure was used to react 2-methyl- and 2-ethylazulene with acetoxymethylpyrroles **19** to generate azulitripyrranes **20a** and **20b** in 75–82% yield (Scheme 3). Azulitripyrranes **20a** and **20b** were purified by column chromatography on silica gel and following recrystallization from chloroform-hexanes were isolated as deep blue powders. The symmetry of these structures was evident from the proton and carbon-13 NMR spectra. For **20a**, the proton NMR spectrum (Fig. 3) showed the azulene protons as a 2H doublet at 8.12 ppm, a 1H triplet at 7.51 ppm and a 2H triplet at 7.10 ppm. The bridging methylene units appeared at 4.31 ppm, while the azulene methyl substituent showed up at 2.35 ppm.

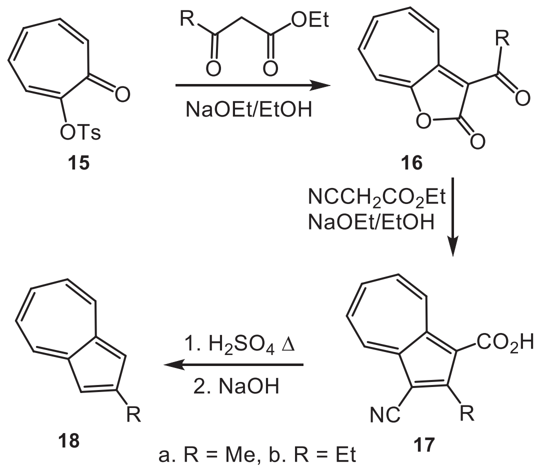

Scheme 2. Synthesis of 2-alkylazulenes

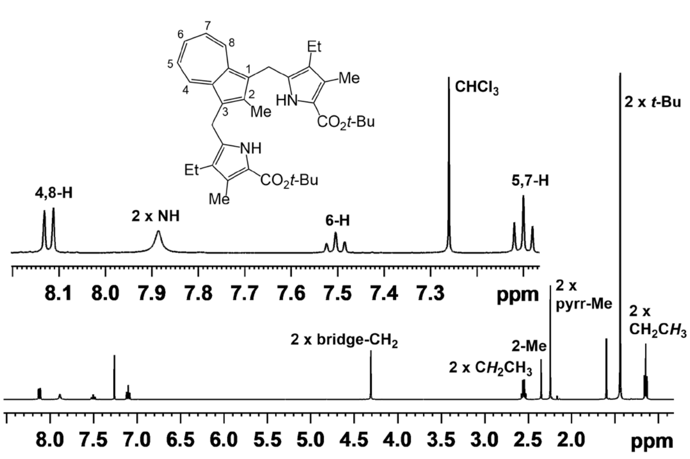

Fig. 3. 500 MHz proton NMR spectrum of 2-methylazulitripyrrane **20a** in $CDCl_3$

Azulitripyrrane **20a** was treated with TFA to cleave the *tert*-butyl ester protective groups, and the solution was then diluted with dichloromethane and reacted with pyrrole dialdehyde **21**. However, following oxidation with ferric chloride or DDQ, the targeted 21-methylazuliporphyrin could not be isolated. Further experimentation indicated that 21-alkyl azuliporphyrin free bases are unstable and the preparative procedure was adjusted to take this factor into account. Hence, after **20a** had been stirred with TFA for 10 min, the deprotected intermediate **22** was reacted with **21** in acetic

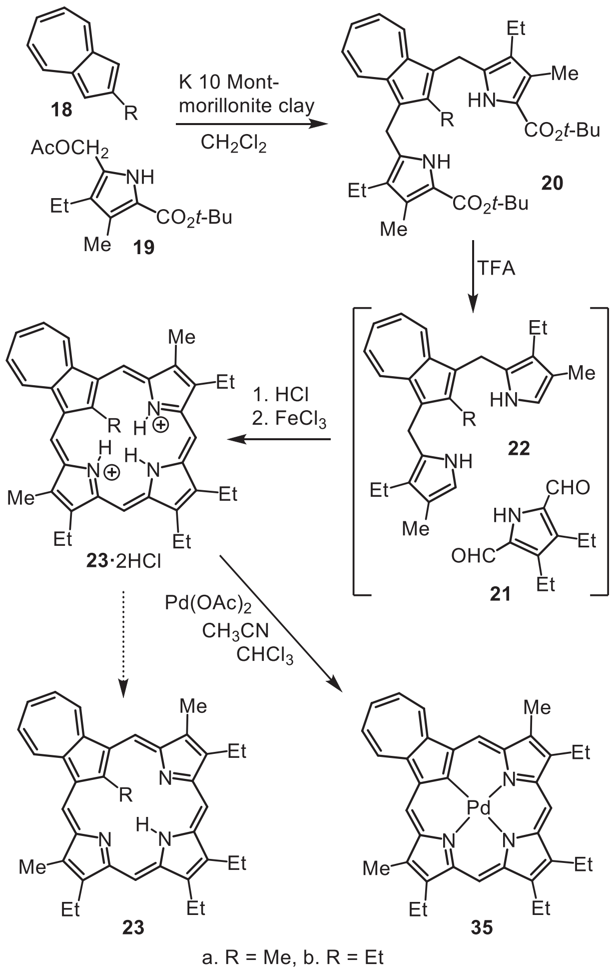

Scheme 3. Synthesis and metalation of 21-alkylazuliporphyrins

acid containing catalytic hydrochloric acid. Following oxidation with aqueous ferric chloride, pure 21-methylazuliporphyrin dihydrochloride **23a**·2HCl could be isolated in 61% yield as a green solid following two recrystallizations from chloroform-hexanes. The diprotonated form appeared to be stable, although attempts to purify the compound by column chromatography were unsuccessful. Azulitripyrrane **20b** reacted similarly to give 21-ethylazuliporphyrin **23b**·2HCl.

Characterization of 21-alkylazuliporphyrins proved to be challenging. NMR data could not be obtained in most organic solvents, including $CDCl_3$, but dilute solutions in DMSO-d_6 did afford proton NMR spectra. At higher concentrations, severe line broadening occurred, and it was not possible to obtain carbon-13 NMR spectra. The proton NMR spectra of the dications showed that the system is strongly diatropic and the internal methyl resonance for **23a** was shifted upfield to -3.6 ppm. The external *meso*-protons were similarly located downfield, giving two 2H singlets at 8.99 (10,15-H) and 10.23 (5,20-H) ppm. The internal ethyl unit for **23b** was similarly shielded, giving a broad 2H quartet at -3.79 ppm and a broad 3H triplet at -2.01 ppm (Fig. 4). The methylene units for the external ethyl groups of **23a** and **23b** were highly diastereotopic giving rise to complex multiplets between 3.5 and 4.1 ppm and this effect results from a loss of symmetry due to the internal alkyl unit residing on one side of the porphyrinoid macrocycle. HSQC spectra could be obtained over a period of several hours and these provided some carbon-13 data. The *meso*-carbons for **23a** appeared at 95.4 (10,15-CH) and 107.0 (5,20-CH) ppm.

The UV-vis spectrum for **23b**·2HCl in chloroform gave two Soret-like bands at 376 and 458 nm and several broad absorptions between 600 and 800 nm (Fig. 5). Addition of TFA led to a slight intensification of the Soret bands, together with minor shifts, and these changes were attributed to hydrogen bonding interactions. Addition of triethylamine to a solution of **23b**·2HCl led to drastic changes due to the formation of the unstable free-base structure (Fig. 5). When the spectrum was recorded immediately after the addition, several weakened bands were observed between 350 and 500 nm, together with broad absorptions at higher wavelengths (Fig. 5). On standing, the UV-vis spectrum slowly changed (Fig. 6) but no specific products could be identified from this degradative process. Similar observations were made for **23a**·2HCl.

Syntheses of 23-methylazuliporphyrins **24** were attempted by reacting *N*-methyltripyrrane **11** [29] with azulene dialdehydes **25a** and **25b** (Scheme 4). Once again, the resulting azuliporphyrins appeared to be unstable in the free-base forms and it was necessary to isolate the products as dicationic species. The best results were obtained by reacting **11** with azulene dialdehydes in TFA-dichloromethane and oxidizing the crude products with aqueous ferric chloride. Following treatment with 10% hydrochloric acid and recrystallization (×2) from chloroform-hexanes, the azuliporphyrin dihydrochlorides were obtained as dark green solids. Unfortunately, NMR data could not be obtained for **24a** and our study focused on the *tert*-butyl substituted derivative **24b**. Even then, azuliporphyrin dihydrochloride **24b**·2HCl only gave a satisfactory proton NMR spectrum in TFA-DMSO-d_6 (Fig. 7). The dication showed strongly aromatic features as the internal 21-H and 23-methyl resonances were shifted upfield to give singlets at -3.54 and -3.48 ppm, respectively. The NH protons appeared at -0.57 ppm, while the *meso*-protons afforded two downfield 2H singlets at 9.46 (10,15-H) and 10.44 (5,20-CH) ppm. The methylene protons for the ethyl substituents were again diasterotopic, giving rise to complex multiplets between 3.35 and 3.76 ppm. A carbon-13 NMR spectrum could be obtained at 60 °C and this showed the N-Me at 32.4 ppm, the internal CH at 125.8 ppm, and the *meso*-carbons at 97.3 and 111.2 ppm.

The UV-spectra for **24b**·2HCl more closely resembled those for regular azuliporphyrins [30]. In chloroform, two Soret bands are seen at 377 and 476 nm, while

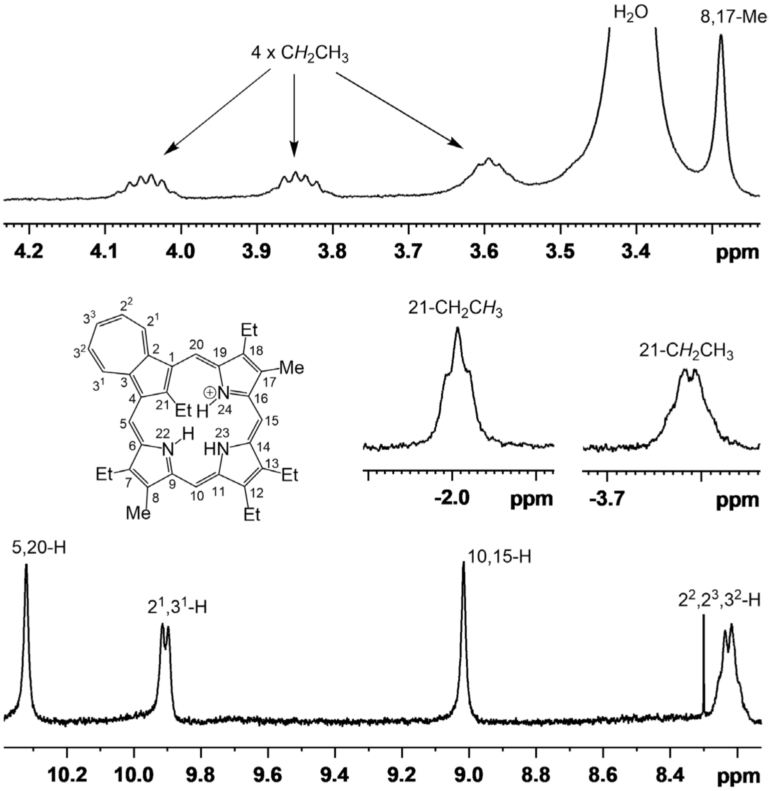

Fig. 4. 500 MHz proton NMR spectrum of 21-ethylazuliporphyrin dihydrochloride **23b**·2HCl in DMSO-d_6

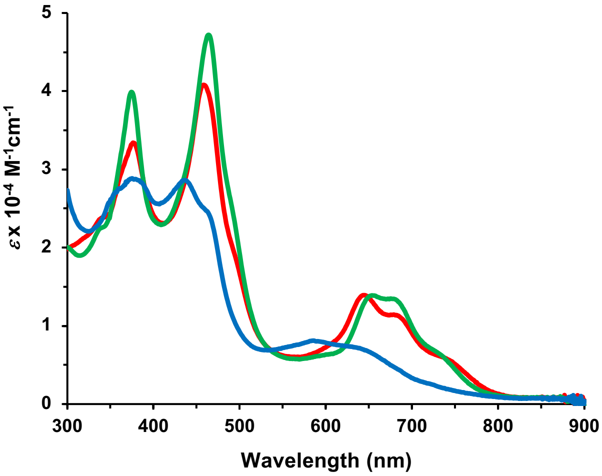

Fig. 5. UV-vis spectra of azuliporphyrin **23b**·2HCl in chloroform (red line), 1% TFA-chloroform (green line) and 1% triethylamine-chloroform (blue line)

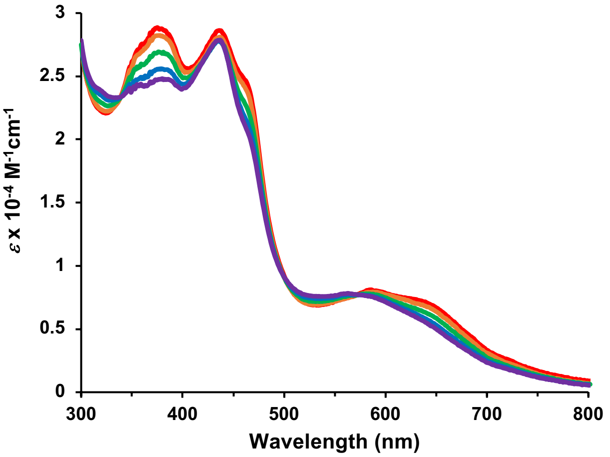

Fig. 6. UV-vis spectra of azuliporphyrin **23b**·2HCl in 1% triethylamine-chloroform showing how the absorptions change with time. Red line: spectrum immediately after addition of Et$_3$N. After 5 min (orange), 20 min (green), 40 min (blue) and 60 min (purple)

several weaker bands are seen between 590 and 800 nm (Fig. 8). Addition of TFA led to minor hypsochromic shifts to the Soret bands and a slight intensification of the absorptions, most likely due to hydrogen bonding interactions. In 1% triethylamine-chloroform, a typical azuliporphyrin-type spectrum was obtained showing four bands in the Soret region at 364, 402, 457 and 484 nm, together with a broad absorption at higher wavelengths (Fig. 8). These values are all bathochromically shifted compared to an analogous azuliporphyrin lacking the internal alkyl substituent [56]. The structures of **23a, 23b** and **24b** were supported by high resolution electrospray ionization (ESI) mass spectrometry.

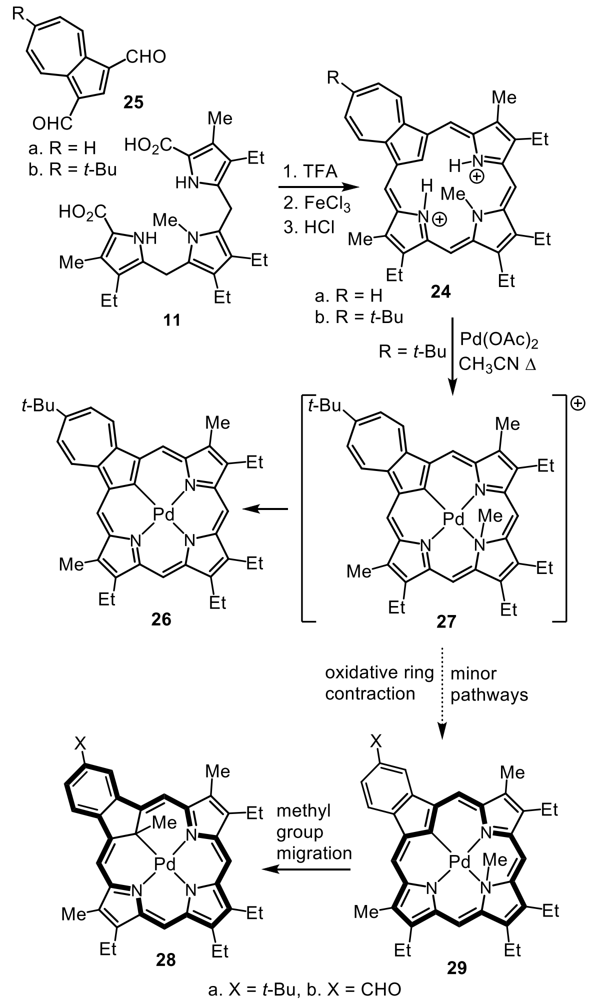

Scheme 4. Synthesis and metalation of a 23-methylazuliporphyrin

In order to investigate how alkylation within the porphyrinoid cavity affects metalation processes, reactions with palladium(II) acetate were investigated. When 21-methylazuliporphyrin **24b**·2HCl was heated with palladium(II) acetate and sodium acetate in chloroform-acetonitrile, the main product was palladium(II) azuliporphyrin **26**. Closely related structures have previously been prepared from *N*-unsubstituted azuliporphyrins [38a, 38b, 56]. The identity of the product was established by NMR spectroscopy and high resolution ESI mass spectrometry. Both the proton and carbon-13 NMR spectra showed that the product retained a plane of symmetry and the *meso*-protons were observed as two 2H singlets at 8.68 and 9.26 ppm. However, the metalloporphyrinoid no longer possesses an internal alkyl substituent. Initially, TLC analysis of the reaction solution showed that a polar derivative had been formed and this was tentatively attributed to **27**. S_N2 displacement of the methyl group, where the palladium(II) complex is effectively the leaving group, presumably explains the final result and similar observations have previously been made for *N*-alkylporphyrins [62, 63]. Several minor products were also observed, two of which could be identified. The byproducts were purified by column chromatography and an initial green fraction was collected consisting of two different compounds. Further chromatographic purification of the early material, eluting with 25% dichloromethane-hexanes, gave an unidentified green fraction followed by an olive-green solution. The proton NMR spectrum of the latter fraction (Fig. 9) showed a loss of symmetry and mass spectrometry indicated that one of the original carbons was missing, although a palladium ion had been incorporated. The internal methyl group was still present, giving rise to a 3H singlet

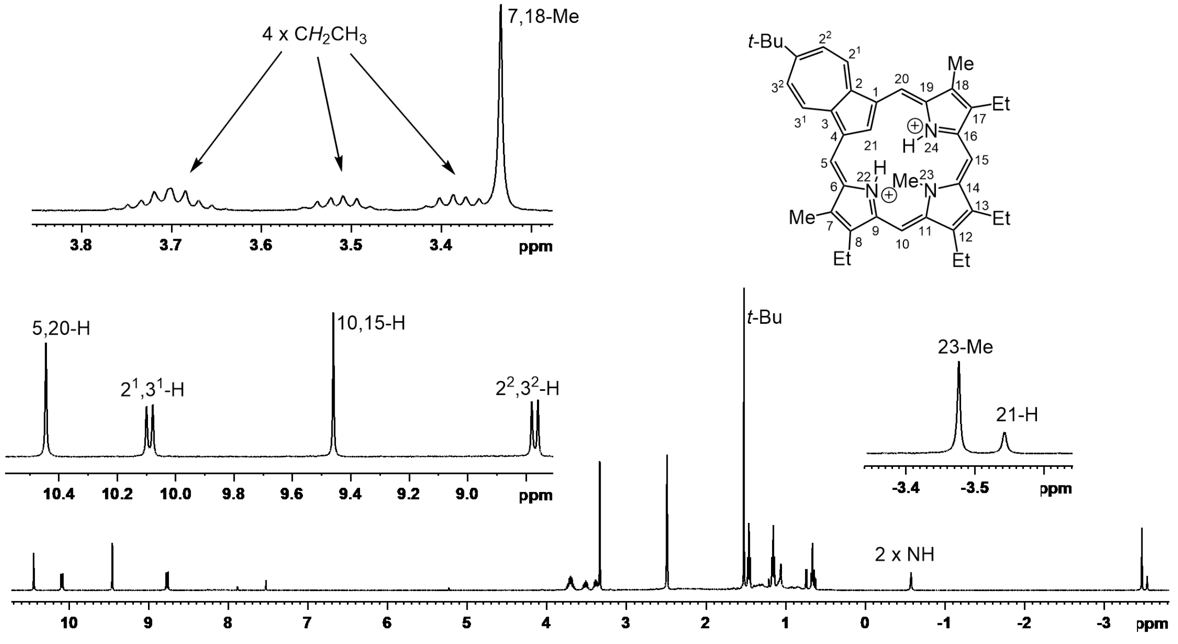

Fig. 7. 500 MHz proton NMR spectrum of **24b**H_2^{2+} in TFA-DMSO-d_6

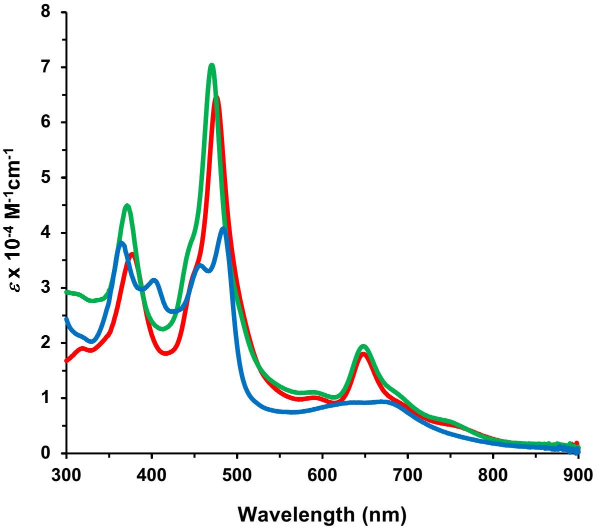

Fig. 8. UV-vis spectra of **24b**H$_2^{2+}$ in chloroform (red line), 1% TFA-chloroform (green line) and 1% triethylamine-chloroform (free base **24b**, blue line)

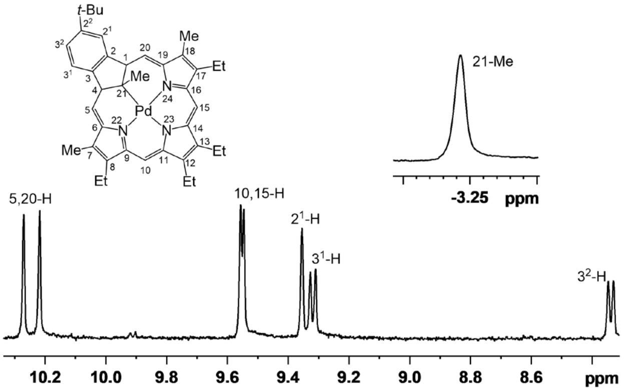

Fig. 9. Partial 500 MHz proton NMR spectrum of palladium(II) *tert*-butylbenzocarbaporphyrin **28a** in CDCl$_3$

at -3.24 ppm. The external protons gave five downfield singlets, four of which corresponded to *meso*-protons. In addition, two doublets with coupling constants J = 8.5 Hz were also observed at 8.34 and 9.32 ppm that were consistent with the presence of a benzene ring. The singlet at 9.36 ppm was also attributed to an arene proton. The strongly deshielded benzene protons demonstrate that the global ring current runs through the exterior of the benzene ring, indicating that the methyl substituent must have migrated onto C-21 [29]. Hence, the results show that palladium(II) benzocarbaporphyrin **28a** had been generated, although this compound was only isolated in 2.4% yield (Scheme 4). In the first column, a brown fraction followed the major product **26** and this compound proved to be a related palladium(II) benzocarbaporphyrin carbaldehyde **28b**. The high resolution ESI mass spectrum showed that the *tert*-butyl substituent had been lost and that an oxygen atom had been incorporated in addition to a palladium cation. The proton NMR spectrum showed that the symmetry of the system had been lost, and the internal methyl group was observed at -3.20 ppm (Fig. 10). Six 1H singlets were observed in the downfield region, one of which was attributed to the formation of an aldehyde unit. Two arene-type doublets (J = 8.2 Hz) were observed at 8.71 and 9.50 ppm, and a singlet at 9.90 ppm was assigned as an isolated benzene proton. The *meso*-protons were observed as four 1H singlets at 9.58, 9.61, 10.36 and 10.39 ppm. Again, the macrocyclic conjugation pathway appears to involve a 22π-electron circuit that passes through the fused benzo-unit and this implies that the *N*-methyl substituent has migrated to the internal carbon [29]. The formation of **28b** is intriguing, but it should be noted that this product was only obtained in 5% yield.

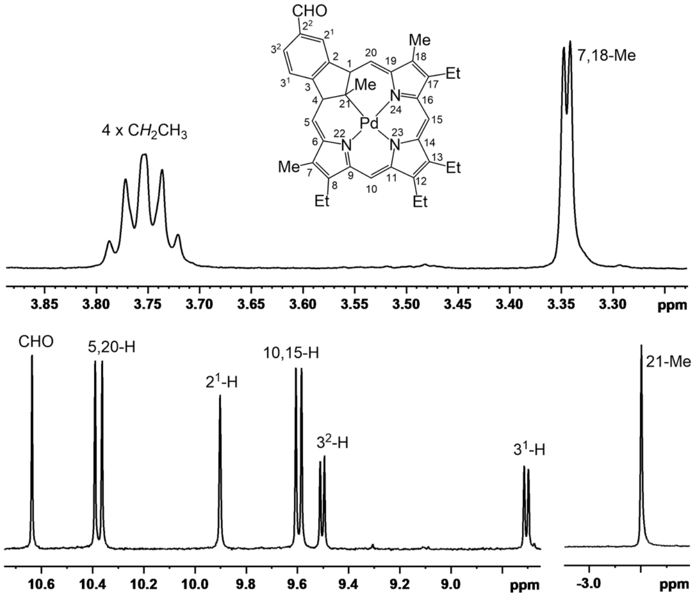

Fig. 10. Partial 500 MHz proton NMR spectrum of palladium(II) benzocarbaporphyrin carbaldehyde **28b** in CDCl$_3$

The UV-vis spectra for **28a** and **28b** (Fig. 11) were similar to related palladium(II) benzocarbaporphyrin complexes [29]. *tert*-Butyl complex **28a** gave two Soret-like bands at 348 and 423 nm, and a long wavelength absorption appeared at 694 nm. These absorptions were present at 346, 429 and 715 nm, respectively, for **28b**. The observed bathochromic shifts for **28b** are consistent with the formyl auxochrome being directly connected to the porphyrinoid chromophore, supporting the proposal that a 22π-electron delocalization pathway is favored in these structures.

It is well known that azuliporphyrins are prone to ring contraction reactions that afford benzocarbaporphyrins [35, 40, 41] and that the

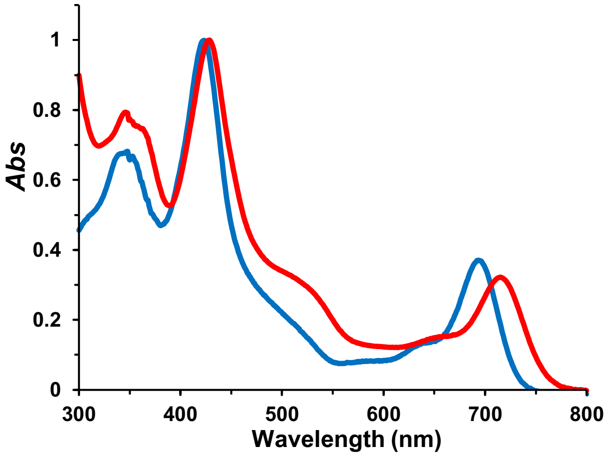

Fig. 11. UV-vis spectra of palladium(II) benzocarbaporphyrins **28a** (blue line) and **28b** (red line) in chloroform

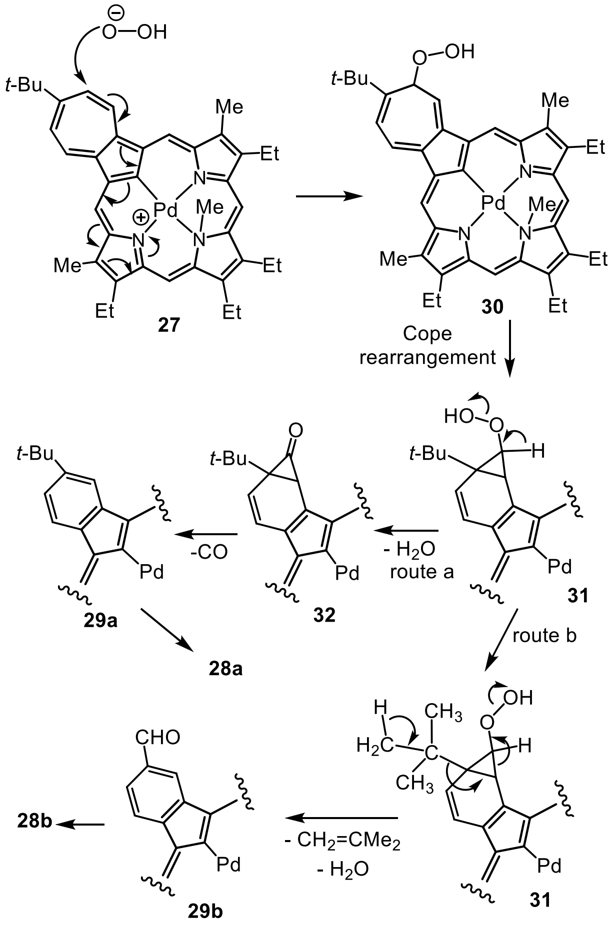

Scheme 5. Proposed mechanisms for the formation of palladium(II) carbaporphyrins

presence of *tert*-butyl substituents does not impede these reactions [56, 64]. It is proposed that initial ring contraction leads to the formation of palladium(II) 23-methyl benzocarbaporphyrins **29** and subsequent alkyl group migration [29] leads to the observed products.

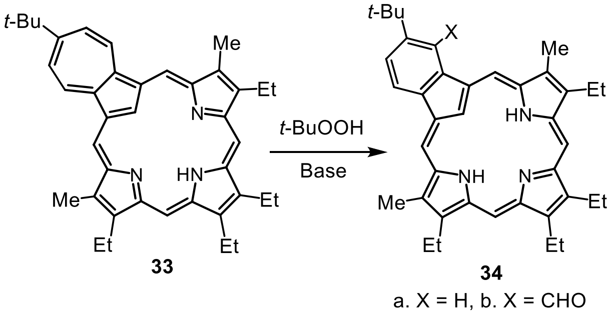

Scheme 6. Ring contraction of a *tert*-butyl substituted azuliporphyrin

Ring contractions of azuliporphyrins have generally been carried out in the presence of peroxides under basic conditions [40]. It has been reported that palladium can induce the formation of peroxides from molecular oxygen [65] and the first step leading to the formation of palladium(II) benzocarbaporphyrins may involve nucleophilic attack from a hydroperoxide ion onto **27** to give **30** (Scheme 5). Cope rearrangement would generate a six-membered ring while closing off a cyclopropane unit affording **31**. Elimination of water would produce cyclopropanone **32** and subsequent extrusion of carbon monoxide would generate palladium(II) 23-methyl *tert*-butylbenzocarbaporphyrin **29a**. This would be expected to undergo a methyl group migration to afford the observed product **28a**. Alternatively, intermediate **31** could undergo elimination of isobutylene and water to produce **29b** and this would further rearrange to produce the observed aldehyde **28b**. Although these proposed mechanisms are reasonable, it should be noted that *tert*-butylazuliporphyrin **33** was reported to undergo ring contractions in the presence of *tert*-butyl hydroperoxide and KOH or *t*-BuOK to give *tert*-butylbenzocarbaporphyrin **34a** and the related aldehyde **34b** [56] (Scheme 6). No loss of the *tert*-butyl group was noted and a palladium complex with the substitution pattern found in **34b** could not be identified in the current investigation. At present, we do not have an explanation for these observations.

Reaction of C-alkylazuliporphyrins **23**$\cdot$2HCl with palladium(II) acetate gave less satisfactory results (Scheme 3). Column chromatography gave rise to two fractions, the first of which corresponded to a brown colored solution. Proton NMR spectroscopy showed that this consisted on a complex mixture of products, although it was notable that multiple peaks were observed downfield between 9.5 and 10.9 ppm and upfield near -4 ppm. Hence, strongly aromatic structures appear to have been generated. Unfortunately, it was not possible to characterize these materials. The second green-brown fraction corresponded to palladium(II) azuliporphyrin **35** where the internal methyl group had been lost. Both **23a** and **23b** gave this system in only *ca.* 10% yield, and as similar derivatives are easily prepared from regular azuliporphyrins [38a,b], this chemistry has little value. Nevertheless, the results do provide some insights into the reactivity of these internally alkylated structures.

CONCLUSIONS

Synthetic routes to internally alkylated azuliporphyrins have been developed. Azulitripyrranes were prepared in good yields by reacting 2-methyl- or 2-ethylazulene with two equivalents of an acetoxymethylpyrrole in the presence of K 10 Montmorillonite clay. Cleavage of the *tert*-butyl esters with trifluoroacetic acid, followed by condensation with a pyrrole dialdehyde in the presence of hydrochloric acid, gave excellent yields of 21-alkylazuliporphyrin dihydrochlorides. However, the free-base azuliporphyrins proved to be unstable and could not be isolated. Reaction of an *N*-methyltripyrrane with azulene dialdehydes in TFA-dichloromethane, followed by oxidation with ferric chloride, gave 23-methylazuliporphyrins that could only be isolated in protonated form. The *tert*-butyl substituted product was sufficiently soluble to allow characterization and proved to have a strong aromatic ring current. Reaction with palladium(II) acetate primarily resulted in demethylation to give a palladium(II) azuliporphyrin, but palladium(II) complexes of ring contracted benzocarbaporphyrins were also observed. Clearly, internal alkylation of carbaporphyrinoids leads to unexpected changes in the reactivity of these systems, and this strategy is likely to be a productive tool when applied to future investigations into porphyrin analogues.

Acknowledgments

This work was supported by the National Science Foundation under grants CHE-1465049 and CHE-1855240.

Supporting information

Selected ^{1}H NMR, ^{1}H–^{1}H COSY, HSQC, DEPT-135, ^{13}C NMR, and UV-vis spectra are provided. This information is available free of charge *via* the internet at http://www.worldscinet.com/jpp/jpp.shtml.

REFERENCES

1. *Porphyrins and Metalloporphyrins*, ed. Smith KM, Elsevier: Amsterdam, 1975, pp 20–24.
2. Cheprakov AV. In *Handbook of Porphyrin Science — With Applications to Chemistry, Physics, Material Science, Engineering, Biology and Medicine*. Smith KM, Kadish KM and Guilard R. (Eds.) World Scientific Publ.: Singapore, 2011, Vol. 13, pp. 1–149.
3. Lash TD. *J. Porphyrins Phthalocyanines* 2001; **5**: 267–288.
4. Sarma T and Panda PK. *Chem. Rev.* 2017; **117**: 2785–2838.
5. Lindsey JS. *Chem. Rev.* 2015; **115**: 6534–6620.
6. Brückner C, Samankumara L and Ogikubo J. In *Handbook of Porphyrin Science — With Applications to Chemistry, Physics, Material Science, Engineering, Biology and Medicine*. Smith KM, Kadish KM and Guilard R. (Eds.) World Scientific Publ.: Singapore, 2012, Vol. 17, pp. 1–112.
7. Chaterjee T, Shetti VS, Sharma R and Ravikanth M. *Chem. Rev.* 2017; **117**: 3254–3328.
8. Brückner C, Akhigbe J and Samankumara LP. In *Handbook of Porphyrin Science — With Applications to Chemistry, Physics, Material Science, Engineering, Biology and Medicine*. Smith KM, Kadish KM and Guilard R. (Eds.) World Scientific Publ.: Singapore, 2014, Vol. 31, pp. 1–275.
9. Lash TD. In *Handbook of Porphyrin Science — With Applications to Chemistry, Physics, Material Science, Engineering, Biology and Medicine*. Smith KM, Kadish KM and Guilard R. (Eds.) World Scientific Publ.: Singapore, 2012, Vol. 16, pp. 1–329.
10. Lash TD. *Chem. Rev.* 2017; **117**: 2313–2446.
11. Paolesse R. In *The Porphyrin Handbook*. Smith KM, Kadish KM and Guilard R. (Eds.) Academic Press: San Diego, CA, 2000, Vol. 2, pp. 201–232.
12. Orlowski R, Gryko D and Gryko DT. *Chem. Rev.* 2017; **117**: 3102–3137.
13. Inokuma Y and Osuka A. *Dalton Trans.* 2008; **37**: 2517–2526.
14. Shimizu S. *Chem. Rev.* 2017; **117**: 2730–2784.
15. Sessler JL and Seidel D. *Angew. Chem., Int. Ed.* 2003; **42**: 5134–5175.
16. Tanaka T and Osuka A. *Chem. Rev.* 2017; **117**: 2584–2640.
17. Lavallee DK. *The Chemistry and Biochemistry of N-Substituted Porphyrins*. VCH: New York, 1987.
18. (a) Lavalee DK and Gebala A. *Inorg. Chem.* 1974; **13**: 2004–2008. (b) Al-Hazimi HMG, Jackson AH, Johnson AW and Winter M. *J. Chem. Soc., Perkin Trans.* 1 1977: 98–103.
19. (a) Jackson AH, Pandey RK and Roberts E. *J. Chem. Soc., Chem. Commun.* 1985: 470–471. (b) Pandey RK, Jackson AH and Smith KM. *J. Chem. Soc., Perkin Trans.* 1 1991: 1211–1220.
20. Bain-Ackerman MJ and Lavallee DK. *Inorg. Chem.* 1977; **18**: 3358–3364.
21. De Matteis F, Gibbs AH and Holley AE. *Ann. New York Acad. Sci.* 1987; **514**: 30–40.
22. (a) Chmielewski PJ and Latos-Grażyński L. *J. Chem. Soc., Perkin Trans.* 2 1995: 503–509. (b) Xiao Z and Dolphin D. *Tetrahedron* 2002; **58**: 9111–9116.
23. Sahota, N, Ferrence GM and Lash TD. *J. Org. Chem.* 2017; **82**: 9715–9730.
24. Lash TD. *Org. Lett.* 2011; **13**: 4632–4635.
25. Lash TD, Miyake K, Xu L and Ferrence GM. *J. Org. Chem.* 2011; **76**: 6295–6308.

26. Lash TD and Rooney JM. *J. Porphyrins Phthalocyanines*, in press. DOI: 10.1142/S1088424619501098.
27. Grabowski EY, AbuSalim DI and Lash TD. *J. Org. Chem.* 2018; **83**: 11825–11838.
28. Li D and Lash TD. *J. Org. Chem.* 2014; **79**: 7112–7121.
29. Latham AN, Ferrence GM and Lash TD. *Organometallics* 2019; **38**: 575–585.
30. Lash TD. *Acc. Chem. Res.* 2016; **49**: 471–482.
31. Lash TD and Chaney ST. *Angew. Chem., Int. Ed. Engl.* 1997; **36**: 839–840.
32. Lash TD and Hayes MJ. *Angew. Chem. Int. Ed. Engl.* 1997; **36**: 840–842.
33. Lash TD, Hayes MJ, Spence JD, Muckey MA, Ferrence GM and Szczepura LF. *J. Org. Chem.* 2002; **67**: 4860–4874.
34. AbuSalim DI and Lash TD. *J. Phys. Chem. A* 2019; **123**: 230–246.
35. Lash TD, Colby DA, Graham SR and Chaney ST. *J. Org. Chem.* 2004, **69**: 8851–8864.
36. Toganoh M and Furuta H. In *Handbook of Porphyrin Science — With Applications to Chemistry, Physics, Material Science, Engineering, Biology and Medicine*. Smith KM, Kadish KM and Guilard R. (Eds.) World Scientific Publishing: Singapore, 2010; Vol. 2, pp. 103–192.
37. Lash TD. *Chem. — Asian J.* 2014; **9**: 682–705.
38. (a) Graham SR, Ferrence GM and Lash TD. *Chem. Commun.* 2002; **38**: 894–895. (b) Lash TD, Colby DA, Graham SR, Ferrence GM and Szczepura LF. *Inorg. Chem.* 2003; **42**: 7326–7338. (c) Lash TD, Pokharel K, Zeller M and Ferrence GM. *Chem. Commun.* 2012; **48**: 11793–11795. (d) Stateman LM, Ferrence GM and Lash TD. *Organometallics* 2015; **34**: 3842–3848. (e) Bialek M and Latos-Grażyński L. *Chem. Commun.* 2014; **50**: 9270–9272.
39. (a) Colby DA, Ferrence GM and Lash TD. *Angew. Chem., Int. Ed.* 2004; **43**: 1346–1349. (b) Adiraju VAK, Ferrence GM and Lash TD. *Org. Biomol. Chem.* 2016; **14**: 10523–10533.
40. Lash TD. *Chem. Commun.* 1998; **34**: 1683–1684.
41. (a) Colby DA and Lash TD. *Chem. Eur. J.* 2002; **8**: 5397–5402. (b) Lash TD, Colby DA and Ferrence GM. *Eur. J. Org. Chem.* 2003: 4533–4548.
42. Noboa MA, AbuSalim DI and Lash TD. *J. Org. Chem.* 2019: **84**: 11649–11664.
43. Richter DT and Lash TD. *J. Org. Chem.* 2004; **69**: 8842–8850.
44. Larsen S, McCormick-McPherson LJ, Teat SJ and Ghosh A. *ACS Omega* 2019; **4**: 6737–6745.
45. (a) Zhang Z, Ferrence GM and Lash TD. *Org. Lett.* 2009; **11**: 101–104. (b) Sprutta N, Świderska M and Latos-Grażyński L. *J. Am. Chem. Soc.* 2005; **127**: 13108–13109. (c) Sprutta N, Siczek M, Latos-Grażyński L, Pawlicki M, Szterenberg L and Lis T. *J. Org. Chem.* 2007; **72**: 9501–9509. (d) Lash TD, Colby DA, Idate AS and Davis RN. *J. Am. Chem. Soc.* 2007; **129**: 13800–13801. (e) Lash TD, Lammer AD, Idate AS, Colby DA and White K. *J. Org. Chem.* 2012; **77**: 2368–2381. (f) Lash TD, Fosu SC, Smolczyk TJ and AbuSalim DI. *J. Org. Chem.* 2018; **83**: 12619–12631. (g) Ahmad S, Singhal A, Nisa K and Chauhan SMS. *Inorg. Chem.* 2018; **57**: 11333–11340. (h) Sasaki Y, Takase M, Okujima T, Mori S and Uno H. *Org. Lett.* 2019; **21**: 1900–1903.
46. Doering WE and Hiskey CF. *J. Am. Chem. Soc.* 1952; **74**: 5688–5693.
47. Nozoe T, Takase K, Nakazawa T and Fukuda S. *Tetrahedron* 1971; **27**: 3357–3368.
48. Alder RW and Wilshire C. *J. Chem. Soc., Perkin Trans.* 1 1975: 1464–1468.
49. Nozoe T, Takase K, Nakazawa T, Sugita S and Saito M. *Bull. Chem. Soc. Jpn.* 1974; **47**: 1750–1753.
50. Nozoe T, Seto S and Matsumura S. *Bull. Chem. Soc. Jpn.* 1962; **35**: 1990–1998.
51. Wagner-Jauregg T, Arnold H, Huter F and Schmidt J. *Ber. Dtsc. Chem. Ges.* 1941; **74B**: 1522–1528.
52. Plattner PA and Furst A. *Helv. Chim. Acta* 1945; **28**: 1636–1638.
53. Clezy PS, Crowley RJ and Hai TT. *Aust. J. Chem.* 1982; **35**: 411–421.
54. Tardieux C, Bolze F, Gros CP and Guilard R. *Synthesis* 1998: 267–268.
55. Li R, Lammer AD, Ferrence GM and Lash TD. *J. Org. Chem.* 2014; **79**: 4078–4093.
56. Lash TD, El-Beck JA and Ferrence GM. *J. Org. Chem.* 2007; **72**: 8402–8415.
57. Lash TD. *Chem. — Eur. J.* 1996; **2**: 1197–1200.
58. Lash TD. *J. Porphyrins Phthalocyanines* 2016; **20**: 855–888.
59. Iwama N, Kashimoto M, Ohtaki H, Kato T and Sugano T. *Tetrahedron Lett.* 2004; **45**: 9211–9213.
60. Graham SR, Colby DA and Lash TD. *Angew. Chem. Int. Ed.* 2002; **41**: 1371–1374.
61. Okujima T, Kikkawa T, Nakano H, Kubota H, Fukugami N, Ono N, Yamada H and Uno H. *Chem. — Eur. J.* 2012; **18**; 12854–12863.
62. Doi JD, Compito-Magliozzo C and Lavallee DK. *Inorg. Chem.* 1984; **23**: 79–84.
63. Stinson C and Hambright P. *Inorg. Chem.* 1976; **15**: 3181–3182.
64. El-Beck JA and Lash TD. *Eur. J. Org. Chem.* 2007: 3981–3990.
65. Yi H and Lei A. *Chem. — Eur. J.* 2017; **23**: 10023–10027.